J. Membrane Biol. 161, 21–32 (1998)

The Journal of
Membrane
Biology

Electrorotation of Isolated Generative and Vegetative Cells, and of Intact Pollen Grains of *Lilium longiflorum*

V.L. Sukhorukov[1], R. Benkert[2], G. Obermeyer[2], F.-W. Bentrup[2], U. Zimmermann[1]

[1]Lehrstuhl für Biotechnologie der Universität Würzburg, Biozentrum, Am Hubland, D-97074 Würzburg, Germany
[2]Institut für Pflanzenphysiologie der Universität Salzburg, Hellbrunnerstr. 34, A-5020 Salzburg, Austria

Received: 9 June 1997/Revised: 4 August 1997

Abstract. The dielectric structure of mature pollen of the angiosperm *Lilium longiflorum* was studied by means of single-cell electrorotation. The use of a microstructured four-electrode chamber allowed the measurements to be performed over a wide range of medium conductivity from 3 to 500 mS m^{-1}. The rotation spectra of hydrated pollen grains exhibited at least three well-resolved peaks in the kHz-MHz frequency range, which obviously arise due to the multilayered structure of pollen grains. The three-shell model can explain the complex rotational behavior of pollen grains in terms of conductivities, permittivities and thicknesses of the following compartments: the exine and intine of the pollen grain wall as well as the membrane and cytoplasm of the vegetative cell. However, the number of unknown parameters (more than 8) was too large to allow unambiguous values to be assigned to any of them. Therefore, to facilitate the evaluation of the pollen grain parameters, additional rotational measurements were made on isolated vegetative and generative cells. The rotation spectra of these cells could be fitted very accurately on the basis of the single-shell model by assuming a dispersion of the cytoplasm. The data on the membrane and cytoplasmic properties of isolated vegetative cells were then used for modeling the rotation spectra of pollen grains. This greatly facilitated the fitting of the theoretical model to the experimental data and allowed the dielectric properties of the major structural units to be determined. The dielectric characterization of pollen is of enormous interest for plant biotechnology, where pollen and isolated germ cells are successfully used for production of transgenic crop and drug plants of economic importance by means of electromanipulation techniques.

Correspondence to: U. Zimmermann

Key words: *Lilium longiflorum* — Pollen grain — Protoplast — Vegetative cell — Generative cell — Electrorotation — Microstructure — Dispersion

Introduction

Germinating pollen grains from various plants and particularly from the angiosperm *Lilium longiflorum* have proved to be very useful model systems for studying the molecular mechanisms of the polar tip growth, that is the rapid polarized extension of a single-cell restricted to their apical tips. This phenomenon is observed in many other plant and animal systems, such as algal rhizoids, fungal hyphae, root hairs in higher plants and neurites (Heath, 1995; Obermeyer & Bentrup, 1996; Heidemann, 1996). The pollen tube growth involves many cell components including the actomyosin system, movement of the male germ unit, cytoplasmic streaming, fusion of vesicles, regulation of the Ca^{2+}- and H^+-concentrations, and activity of the ion transporters located in the plasma membrane of the pollen grain and along the growing pollen tube (Battey & Blackbourn, 1993; Feijó, Malhó & Obermeyer, 1995; Cai, Moscatelli & Cresti, 1997).

Endogenous electric fields precede and accompany the growth of pollen tubes and of other tip-growing cell systems (Harold & Caldwell, 1990). The germinating pollen grain drives a substantial electrical current through itself (with positive charge entering the growing tip (Weisenseel, Nuccitelli & Jaffe, 1975)) and, therefore, can be viewed as a permanent electrical dipole suspended in a conductive medium. The molecular transport mechanisms of the principal charge carriers (Ca^{2+}, K^+ and H^+) responsible for this endogenous electric field have been studied by means of several different experimental techniques, including fluorescent probes (Obermeyer & Weisenseel, 1991; Miller et al., 1992), immu-

nolocalization (Obermeyer et al., 1992) and extracellular vibrational, ion-selective electrodes (Kühtreiber & Jaffe, 1990; Pierson et al., 1995). Ultrastructural and biochemical studies revealed the complex multicellular and multilayered structure of the pollen grains of angiosperms, which is characterized by the unique, generative-within-vegetative cell arrangement (Cresti, Blackmore & Van Went, 1992). In addition, the vegetative cell is enclosed in the wall that fulfills an important protective function and consists of at least two layers (the exine and intine) of very differing chemical composition.

The germinating pollen grains are very sensitive to external AC and DC electric fields, presumably due to their endogenous electrical activity, e.g., the sites of germination of tobacco pollen grains and the direction of tube growth are affected by applied DC electric fields (Wang, Rathore & Robinson, 1989). Exposed to extremely weak alternating electric fields of strength as small as few mV cm^{-1}, the pollen tubes of *Lilium longiflorum* grew more rapidly probably via activation of the P-type H^+ ATPase located in the plasma membrane (Plätzer, Obermeyer & Bentrup, 1997). These results suggest that mobile charges of ion transport systems within the plasma membrane appear to be the most likely target of electric fields. In spite of extensive studies little is known about the role and mechanisms of electrical activity in fast growing pollen tubes of angiosperms, and also about the molecular mechanisms through which external electric fields modulate pollen germination. Additional insight into the mechanisms of generation and interaction of electric fields in germinating pollen grains can be obtained by studying the dielectric structure of pollen, because the electric polarization fields must satisfy the dielectric properties of the target cell and of the surrounding medium. (However, the use of conventional techniques, like patch-clamp and impaled microelectrodes, for studying on intact pollen grains is cumbersome because of the presence of the extremely dense pollen wall.)

Due to the considerable potential of pollen in breeding of crop and drug plants, the dielectric characterization of pollen grains and of isolated gamete cells are of relevance to further exploitation of the electromanipulation techniques (permeabilization and fusion) in plant biotechnology. Recent years have shown that electropermeabilization allows the introduction of foreign macromolecular substances (i.e., plasmids, dextrans) into ungerminated pollen grains of different plants (Mishra, Joshu & Bhatia, 1987; Obermeyer & Weisenseel, 1995; Zimmermann, 1996) and can be successfully used for production of transgenic plants (Saunders, Matthews & Wert, 1992; Saunders et al., 1995). Another approach for transformation of plants is electrofusion of plant cell protoplasts (Zimmermann, 1982; 1986). This is a powerful technique, which combines controlled field-induced permeabilization of the plasma membrane with methods to enhance contact between cells, particularly via dielectrophoresis. Electrofusion can be used not only for somatic, but also for gametosomatic hybridization (a fertilization like process) and for fusion of isolated gametes, i.e., electrofusion-mediated in vitro fertilization (for review *see* Zimmermann (1996)). It is evident, that detailed information on the electrical properties of particular cells (pollen grains, isolated protoplasts etc.) are essential for a better understanding and control of the biophysical parameters involved in electropermeabilization and electrofusion, and for further improvement of the present electromanipulation protocols.

We studied here the dielectric properties of hydrated mature pollen grains of the angiosperm *Lilium longiflorum* by means of the single-cell electrorotation (Arnold & Zimmermann, 1982, 1983). In the last few years, electrorotation has become the principal means used for the dielectric characterization of individual cells (Jones, 1995; Fuhr, Zimmermann & Shirley, 1996; Arnold & Zimmermann, 1988). Theoretical and model investigations show that valuable information not only on the dielectric parameters but also on the ion transport mechanisms in living cells can be obtained (Sukhorukov & Zimmermann, 1996; Nielsen et al., 1996; Wang et al., 1997). It is a noninvasive method and contrasts to conventional dielectric spectroscopy (impedance) which must be performed on very dense cell suspensions.

The extraction of meaningful information from electrorotation spectra of heterogeneous particles, such as multicellular and multilayered pollen grains, is not straightforward, because each dielectric composing the pollen grain may yield an additional maximum in the rotation spectrum. Therefore, to facilitate the interpretation of the complex electrorotational behavior of intact pollen grains, we isolated the major structural units of the pollen grain, i.e., the vegetative cell (hereafter the protoplast) and the generative cell, and studied their individual dielectric properties.

Materials and Methods

Isolation of Protoplasts from Pollen Grains

Pollen grains were collected from fully developed flowers of *Lilium longiflorum* Thunb. and used either immediately for the experiments or were frozen in liquid nitrogen and then stored at −20°C. For protoplast isolation we used the procedure according to Tanaka (1988). Pollen grains from one anther of *Lilium longiflorum* Thunb. were suspended in 1 ml of medium A (10% sucrose, 1 mM KCl, 0.1 mM $CaCl_2$, 1.6 mM boric acid, pH 5.6) and shaken for 5 min. After centrifugation at 50 × *g*, the pollen grains were resuspended and washed once with medium B (in mM 680 mannitol, 5 $CaCl_2$, 10 KCl, 0.5 Na-ascorbate, 10 MES (2-[N-Morpholino]ethanesulfonic acid); the pH was adjusted to 6.0 with BTP (1,3-bis[tris(Hydroxymethyl)methylamino]-propane). The pollen grains were then treated with an enzyme solution (1% pectinase,

2% cellulase and 0.5% maceroxyme) dissolved in medium B. The suspension was gently shaken for about two hours at 25°C and then centrifuged at 50 × *g* at 4°C for about 5 min, so that the vegetative-cell-protoplasts hatched out of the exine. The released protoplasts were washed twice with medium B (centrifugation at 50 × *g*, 4°C, 5 min). The final suspension was layered on the top of a discontinuous sucrose (0.8/0.4 M) gradient. After centrifugation (50 × *g*, 4°C, 10 min), the purified protoplasts were collected from the interface between the two sucrose concentrations. The protoplasts were allowed to recover for 1–2 hr in the dark on ice before they were used for experiments.

Isolation of Generative Cells

For isolation of generative cells, the vegetative-cell-protoplasts were transferred in distilled water. The protoplasts swelled and finally burst. Additionally, the suspension was gently homogenized to open the protoplasts. The released generative cells were washed 3 times with medium A (centrifugation at 500 × *g*, 4°C, 3 min). The suspension was then layered on the top of a discontinuous Percoll gradient (20/30%) containing medium A. Following centrifugation (500 × *g*, 4°C, 5 min), the generative cells were collected from the interface between the two Percoll concentrations and washed twice with medium A. The generative cells, which are originally spindle-shaped within the vegetative cell cytoplasm (Tanaka, Nakamura & Miki-Hirosige, 1989), became spherical soon after liberation and were suitable for electrorotation measurements.

All salts were obtained from Merck (Darmstadt, Germany). The buffers and pectinase were purchased from Sigma (Taufkirchen, Germany). Cellulase and macerozyme were obtained from Serva (Heidelberg, Germany).

Electrorotation Experimentals

Pollen grains, protoplasts and generative cells were suspended in 700 mOsm mannitol solution containing appropriate amounts of MES/H_2SO_4 (pH 5.6) to adjust the conductivity (at 20–22°C) to 2–500 mS m^{-1}.

Electrorotation spectra were measured in a microstructured four-electrode chamber developed by G. Fuhr (Humboldt-University, Berlin, Germany). The microstructured chamber, which was made by semiconductor technology (Fuhr et al., 1996), was arranged as a planar array of circular electrodes of 60 μm diameter, 1 μm thickness and 400 μm electrode spacing. The miniaturization of the electrodes and the associated improvement of heat-dissipating properties allowed the use of relatively low voltages (compared to the macroscopic electrode chamber, *see* below) and high-conductivity solutions. The use of a microstructured rotation chamber enabled a large scale variation of the medium conductivity from 2 mS m^{-1} to a high conductivity of about 0.5 S m^{-1}. The electrodes were driven by four 90° phase-shifted, symmetrical rectangular signals from a computer-controlled pulse generator HP 8130A (Hewlett-Packard, Boeblingen, Germany) with 2–4 V_{PP} amplitude over the frequency range from 100 Hz to 150 MHz. All rotation spectra were normalized to the driving voltage of 2 V_{PP} in accordance with Eq. 2 (*see* below). The rotation speeds measured at field frequencies above 30 MHz were then corrected for the chamber resonance as described elsewhere (Gimsa et al., 1996). For high conductivities of the suspending medium (>30 mS m^{-1}), the correction factors could be obtained by comparison of the theoretical rotation spectrum of Sephadex G15 (Pharmacia Fine Chemicals, Germany) particles with the experimental data. For conductivities less than 20 mS m^{-1}, the rotation spectra are given at frequencies below 30 MHz because correction factors could not be determined.

The field frequency inducing fastest anti-field rotation (f_{c1}) was measured in low-conductivity solutions (2–30 mS m^{-1}) using the macroscopic four-electrode chamber and the contrarotating fields' technique (''null-frequency'' method) which was described in detail by Arnold & Zimmermann (1988). The distance between the planar electrodes (dimensions 1.4 × 1.4 mm, mounted at right angles to each other) was about 1.4 mm. Two opposite electrodes were connected to a conventional conductometer (Knick GmbH, Berlin, Germany) to monitor the conductivity of solutions.

The measured rotation spectra were fitted on the basis of Model 2 or Model 3 (*see* below) using the *Mathematica*® software (Wolfram, 1991). The spectra were corrected by the scaling factor, χ (*see* Eq. 2), that accounts for the poorly characterized local field strength and frictional force experienced by an individual cell (Gascoyne, Becker & Wang, 1995).

Rotation Theory

The imaginary part of the complex Clausius-Mosotti factor (U^*) given by Eq. 1 fully determines the electrorotation spectra of microscopic particles, such as biological cells, protoplasts and polymer spheres (Pastushenko, Kuzmin & Chizmadzhev, 1985; Arnold & Zimmermann, 1988; Schwan, 1988; Gascoyne et al., 1995; Jones, 1995; Fuhr et al., 1996). The polarizability factor U^* is extended from the usual purely dielectric expression to give the following equation:

$$U^* = \frac{\varepsilon_p^* - \varepsilon_e^*}{\varepsilon_p^* + 2\varepsilon_e^*} \tag{1}$$

where ε* is the complex absolute permittivity. The subscripts ''*e*'' and ''*p*'' refer to the external medium and particle, respectively. The steady-state rotation speed (Ω) of a spherical particle is given by:

$$\Omega = -\frac{\varepsilon_e E^2 Im(U^*)}{2\eta} \tag{2}$$

where ε_e and η are the real absolute permittivity and the dynamic viscosity of the medium, respectively; *E* is the strength of the rotating field; $Im(U^*)$ is the imaginary part of the factor U^*. In this study, the value $\chi^2 = \varepsilon_e E^2/(2\eta)$ served as a scaling factor for curve fitting (Gascoyne et al., 1995).

For particles and media with frequency-independent parameters ε (real permittivity) and σ (real conductivity) the complex permittivity is defined as: $\varepsilon^* = \varepsilon - j\sigma/\omega$, where ε and σ are given in [F m^{-1}] and [S m^{-1}], respectively; $j = (-1)^{1/2}$; $\omega = 2\pi f$ is the radian field frequency.

In contrast to homogeneous polymer (e.g., latex or Sephadex) particles, whose rotation spectra exhibit only one peak (Arnold, Schwan & Zimmermann, 1987; Gimsa et al., 1996), the spectra of a biological cell consist of a set of (at least two) co- and antifield rotation maxima. These complex spectra are usually explained by modeling cells as multilayered particles (*see below*). In many cases, the electrical properties of cellular compartments (cell wall, plasma membrane, cytoplasm, vacuole etc.) can be assumed to be frequency-independent (nondispersive models) (Asami & Yonezawa, 1996; Fuhr et al., 1996; Radu et al., 1996).

Single-Shell Nondispersive Model (Model 1)

In the single-shell model, a cell is approximated by a homogeneous, conductive sphere of radius (a) surrounded by shell of thickness (d), corresponding to the membrane. Taking into account that d << a, a simplified expression for the complex permittivity of such a particle

(Eq. 3) can be derived from the original equation of Pauly & Schwan (1959):

$$\varepsilon_p^* = \frac{C_m^* a \cdot \varepsilon_i^*}{C_m^* a + \varepsilon_i^*} \tag{3}$$

where ε_i^* is the complex permittivity of the cytosol; C_m^* is the complex membrane capacitance per unit area given by: $C_m^* = C_m - j\, G_m/\omega$, where $C_m = \varepsilon_m/d$ and $G_m = \sigma_m/d$ are the area specific membrane capacitance [F m^{-2}] and conductance [S m^{-2}], respectively. For a single-shelled particle the theoretical dependence of Ω on field frequency, i.e., rotation spectrum, can be calculated by combining Eqs. 1–3.

On the other hand, if the rotation spectra are considered to be the result of a superposition of two Lorentzian curves (Fuhr & Kuzmin 1986; Fuhr et al. 1996), an expression for the rotation speed of a single-shelled sphere is obtained which contains only noncomplex parameters:

$$\Omega = 2R_1 \frac{(f/f_{c1})}{1 + (f/f_{c1})^2} + 2R_2 \frac{(f/f_{c2})}{1 + (f/f_{c2})^2} \tag{4}$$

The constants R_1 and R_2 in Eq. 4 combine all conductivities, permittivities, the field strength, the thickness of the shell and some other constants (*see* equations noted above). The parameters f_{c1} and f_{c2} are the characteristic frequencies of the fastest anti- and cofield rotation, respectively. The half-width of each rotation peak is at least 1.14 decade of frequency. For low conductivity solutions ($\sigma_e < \sigma_i$), the single-shell model predicts antifield rotation at low frequencies (due to electrical properties of the membrane) and cofield rotation in the MHz-range (due to polarization of the cytosol). Therefore, accurate determination of f_{c1} and f_{c2} allows the calculation of the passive electrical properties of the plasma membrane and the internal conductivity (Fuhr et al., 1996).

For very low-conductivity solutions ($\sigma_i \gg \sigma_e \gg \sigma_m$), the conductivity-dependence of f_{c1} is given by Eq. 5 (Arnold & Zimmermann, 1988; Fuhr et al., 1996):

$$f_{c1} \cdot a = \frac{\sigma_e}{\pi \cdot C_m} + \frac{a \cdot G_m}{2\pi \cdot C_m} \tag{5}$$

According to Eq. 5 the characteristic frequency, f_{c1}, shifts linearly to higher frequencies with increasing external conductivity. Therefore, a plot of the frequency f_{c1} (normalized against radius in order to take into account the variations in size of a cell population) *vs.* the external conductivity, σ_e, should yield a straight line.

Single-Shell Model with Dispersive Cytosol (Model 2)

As shown by electron microscopy, protoplasts of pollen grains of *Lilium longiflorum* contain a large number of differently sized vesicles and organelles (among them a relatively large, spindle-shaped generative cell) (Tanaka, 1988). Combined with the presence of high concentrations of macromolecules, such structural organization could lead to a dispersion of the electrical properties of the cytosol (a frequency dependence of conductivity and permittivity) and might, therefore, give rise to an additional peak in the rotation spectrum (Gimsa et al., 1996; Wang et al., 1997). In this study, an additional antifield rotation peak was resolved in the rotation spectra of protoplasts and generative cells if measurements were performed at relatively high external conductivities. These spectra could not be any longer explained on the basis of Model 1, but they could be approximated very accurately by assuming a cytosolic dispersion. The dispersion can be described by the following relations (Gimsa et al., 1996):

$$\varepsilon_i = \varepsilon_{ih} + \Delta\varepsilon_i \frac{1}{1 + (\omega\tau_d)^{2(1-\alpha)}} \tag{6a}$$

$$\sigma_i = \sigma_{il} + \Delta\sigma_i \frac{(\omega\tau_d)^{2(1-\alpha)}}{1 + (\omega\tau_d)^{2(1-\alpha)}} \tag{6b}$$

where, $\Delta\varepsilon_i = (\varepsilon_{il} - \varepsilon_{ih})$ and $\Delta\sigma_i = (\sigma_{ih} - \sigma_{il})$ are the interrelated dielectric increments; ε_{ih} (σ_{ih}) and ε_{il} (σ_{il}) are the values of the permittivity (conductivity) at high (subscript ''*h*'') and low (subscript ''*l*'') frequencies, $\tau_d = (2\pi f_d)^{-1}$ is the relaxation time and f_d is the characteristic frequency of the dispersion. The parameter α describes a distribution of relaxation times, with $\alpha = 0$ corresponding to a single relaxation time behavior. Introduction of a distribution of relaxation times (or dispersion frequencies) significantly improves the fit of the rotation spectra of the protoplasts, generative cells and intact pollen grains (see below).

Three-Shell Model (Model 3)

In many cases, rotation spectra of cells (e.g., those of pollen grains, *see below*) show additional peaks or ''shoulders'' which cannot be explained on the basis of the single-shell models (Models 1 and 2). On the basis of a morphological analysis of the cells, their rotation spectra can be described by introducing a second, third or fourth shell because any new interface will induce a new peak in the rotation spectrum (Fuhr et al., 1996; Jones, 1995). The total number of separate peaks or shoulders measured at different external conductivities corresponds to the minimum number of different dielectrics or dispersion phenomena of the biological object that have to be considered for a correct modeling.

In this study, the expressions for the complex polarizability (U^*, *see* Eq. 1) of layered spherical particles subjected to a uniform electric field were derived by solving the Laplace equation for the electrostatic potential according to Fuhr et al. (1996) and Jones (1995). The expressions for U^* of multishelled particles (not given here) are much more complicated than those for a homogeneous sphere (Eq. 1) and for the single-shell model (combination of Eqs. 1 and 3).

The rotation spectrum of a multishelled particle consisting of n dielectric layers differing by their electrical characteristics (ε and σ), can also be presented as a superposition of n Lorentzian functions as follows (with the proviso that peaks are not overlapping) (Fuhr et al., 1996):

$$\Omega = \sum_{i=1}^{n} 2R_i \frac{(f/f_{c1})}{1 + (f/f_{c1})^2} \tag{7}$$

Equation 7 means that the rotation spectrum consists of n peaks (positive and negative) centered at their respective, characteristic frequencies (f_{c1}, f_{c2}, ... f_{cn}). As mentioned above, further peaks may appear if some of the particle's dielectric layers show dispersive properties (Eqs. 6*a* and 6*b*).

A reasonable agreement between the rotation theory and the experimental spectra was achieved if the intact pollen grains were modeled as three-shelled particles with the three shells corresponding to 1) the plasmalemma (C_m and G_m), 2) the cell wall (intine, $\varepsilon_{\text{intine}}$ and σ_{intine}), and 3) the outer cuticularized wall (exine, $\varepsilon_{\text{exine}}$ and σ_{exine}). The thickness of exine and intine was estimated from the electron microphotographs (*not shown*). Intact pollen grains were determined by microscopic inspection to be slightly elongated ellipsoids (the average long and short axes of 120 ± 15 and 100 ± 10 μm, respectively).

It was shown theoretically, that calculation of the rotation spectra for slightly elongated cells using *spherical* models does not lead to noticeable errors (Sokirko, 1992; Radu et al., 1996). Therefore, we approximated the pollen grains by a three-shelled spherical particle of the same volume with the effective radius $a_e = (a_1 \cdot a_s^2)^{1/3}$, where a_1 and a_s are the long and short semiaxes of the particle, respectively. As with protoplast experiments, introduction of a cytoplasmic dispersion (Eqs. 6*a* and 6*b*) resulted in a better simulation of the electrorotation spectra of intact pollen grains.

Results

Rotation Spectra of Pollen Protoplasts and Isolated Generative Cells

Low External Conductivity

Under low-conductivity conditions, reliable electrorotation spectra could be measured up to the frequency of 30 MHz (for limitations of the experimental apparatus *see* Materials and Methods). Electrorotation spectra of protoplasts and generative cells obtained at conductivity less than 20 mS m^{-1} are shown in Fig. 1*AB* (curves 1 and 2). At the lowest conductivity used here (3 mS m^{-1}), the fastest anti-field rotation of protoplasts and generative cells occurred at 3.2 kHz and at 9.1 kHz, respectively. In response to an increase in the external conductivity to 19 mS m^{-1}, the antifield peaks were shifted to 14.4 kHz (protoplasts) and 50 kHz (generative cells). For both cell types, field frequencies above 0.5–1 MHz gave co-field rotation, whose peak could not be resolved completely. Table 1 shows size and frequencies of the rotation peaks estimated by fitting Eq. 4 (superposition of two Lorentzian curves) to the rotation spectra, which revealed no additional shoulders or peaks up to 30 MHz. Judging by the correlation coefficients given in Table 1, the rotation spectra of protoplasts and generative cells obtained in low-conductivity solutions satisfy Eq. 4 well. At these low-conductivity conditions, the simplest single-shell model (Model 1) allowed the cellular and membrane parameters to be deduced: for the protoplasts C_m = 8–10 mF m^{-2}, G_m = 50–200 S m^{-2}, σ_i = 0.5–0.7 S m^{-1}, ε_i = 50–60; and for the generative cells C_m = 7–9 mF m^{-2}, G_m = 100–300 S m^{-2}, σ_i = 0.3–0.5 S m^{-1}, ε_i = 60–70 (Fig. 1, curves 1, dashed).

The membrane parameters, C_m and G_m (Fig. 2), were also determined by measuring the radius-normalized f_{c1} frequency in dependence on the external conductivity, using the ''null-frequency'' method. The linear relationship between the $f_{c1} \cdot a$ and σ_e predicted by Eq. 5 was observed in representative samples of protoplasts (n = 200) and generative cells (n = 120) providing that the external conductivity, σ_e, did not exceed 26 mS m^{-1}. The least square linear fits to the data obtained on these two cell types overlap (Fig. 2, solid and dashed lines). The mean C_m values of protoplasts and generative cells extracted from the linear fits are very similar (10.8 and 10.9 mF m^{-2}), whereas their mean G_m values differ markedly (56 and 167 S m^{-2}, respectively). The high linearity of the plots (Fig. 2) rules out the presence of significant dispersion in the membrane of protoplasts and generative cells in the frequency range of 2–20 kHz and 7–60 kHz, respectively. A dispersion in the membrane would cause an upwardly curved plot of $f_{c1} \cdot a$ *vs.* σ_e (Sukhorukov & Zimmermann, 1996). The internal membranes and organelles did not appear to have any significant influence on the shape and position of the anti-field rotation peak measured under these extremely low-conductivity conditions.

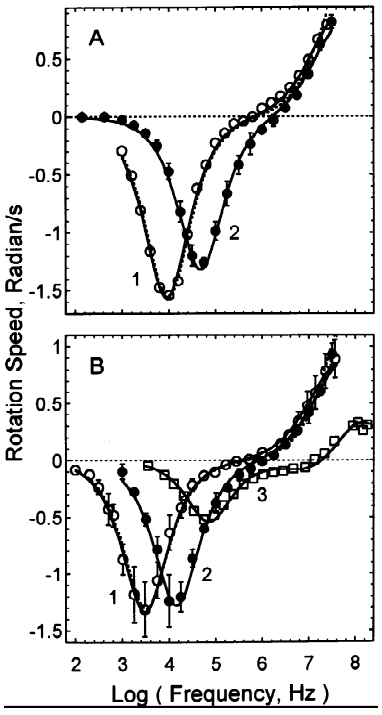

Fig. 1. Experimental electrorotation spectra (symbols) of generative cells (*A*) and protoplasts (*B*) isolated from the pollen of *Lilium longiflorum.* The various curves show best fits of Model 1 (dashed lines) and of Model 2 (solid lines) to the experimental spectra taken at various (relatively low) conductivities of the suspending medium. (*A*) Open and filled circles (curves 1 and 2) show rotation spectra obtained on the isolated generative cells at the external conductivities of 3 and 19 ± 1 mS m^{-1}, respectively. (*B*) Open circles, filled circles and squares (curves 1, 2 and 3) are rotation spectra of the isolated pollen protoplasts at 3, 19 and 166 mS m^{-1}, respectively. The parameters used for curve fitting are summarized in Table 2. Positive values denote cofield rotation.

Taken together, the rotation spectra (Fig. 1) and the $f_{c1} \cdot a/\sigma_e$-data (Fig. 2) on protoplasts and generative cells suggest that under low-conductivity conditions the electrorotational behavior of these cells can be described very accurately by the simplest single-shell model with frequency-invariant properties (Model 1).

Table 1. *The parameters obtained from fitting Eq. 5 and Eq. 7 to the experimental rotation spectra of the pollen grains, protoplasts and generative cells*

σ_e	Radius ± SD μm	*n*	f_{c1} *kHz*	R_1 Radian sec^{-1}	f_{c2} MHz	R_2 Radian sec^{-1}	f_{c3} MHz	R_3 Radian sec^{-1}	f_{c4} MHz	R_4 Radian sec^{-1}	Correlation Coefficient
Generative cells											
3	16	1	9.1	−1.56	28.0	+0.81					0.9991
19 ± 1	15 ± 1	4	50.0	−1.28	44.1	+0.88					0.9991
480 ± 5	15 ± 1	4	414.1	−0.23	15.7	−0.097	(>200)*	(>0)			0.9862
Pollen protoplasts											
3.0 ± 0.4	48 ± 3	7	2.9	−1.3	32.8	+0.87					0.9986
19 ± 1	53 ± 3	3	14.4	−1.23	49.3	+1.02					0.9976
100	49 ± 3	2	48.9	−0.75	1.55	−0.09	110	+0.6			0.9982
166 ± 15	45 ± 2	10	64.7	−0.53	3.72	−0.10	117	+0.32			0.9975
470 ± 10	50 ± 5	5	134.1	−0.27	48.1	−0.19	(>200)	(>0)			0.9787
Pollen grains											
3.0 ± 0.4	50 ± 5	8	8.5	−0.36	0.19	−0.08	17	+0.55			0.9983
19 ± 1.5	53 ± 1	6	14.8	−0.41	0.52	−0.28	40	+0.67			0.9991
186 ± 11	52 ± 1	4	55.2	−0.23	1.54	−0.13	12	−0.15	112	+0.26	0.996
460 ± 10	53 ± 1	3	107	−0.14	4.12	−0.12	92	−0.23	(>200)	(>0)	0.986

* (not resolved peaks)
The driving voltage and the distance between the electrodes were 2 V_{pp} and 400 μm, respectively.

High External Conductivity

When the conductivity of suspending media was adjusted to 100 mS m^{-1} or higher, the rotation speed of the isolated protoplast and generative cells over the whole frequency range became much slower than it was in media with $\sigma_e < 20$ mS m^{-1}. An additional (third) anti-field shoulder (Fig. 1*B*, curve 3) or even a well resolved anti-field peak (Fig. 3) appeared at frequencies above 1 MHz. The single-shell non-dispersive model (Model 1) is no longer applicable in analyzing these rotation spectra, because according to this method only two peaks are expected (*see* Rotation Theory). However, the rotation spectra of both protoplasts and generative cells can be fitted accurately by Eq. 7 (a superposition of three Lorentzian curves) using the fitting parameters (f_{ci}, R_i) listed in Table 1. The deviations from the single-shell model reflect at least one additional dispersion that may arise from structural inhomogenities in the cytosol and from frequency-dependent dielectric properties of cytosolic macromolecules.

The continuous curves in Figs. 1 and 3 are the best-fit theoretical spectra calculated on the basis of Model 2 (a single-shelled cell exhibiting a dispersion of the cytoplasm). The electric parameters used for fitting the data that were obtained over a wide conductivity range (from 2 to about 500 mS m^{-1}) are listed in Table 2 (*see also* legends to Figs. 1 and 3). For protoplasts, the G_m-values estimated from the spectra measured at different conductivities exhibit higher scatter (from 50 to 400 S m^{-2}), which results from the relatively poor accuracy of G_m determination, and is typical for electrorotation (Fuhr et al., 1996). The C_m-values and the cytoplasmic parameters used for curve-fitting vary slightly (Table 2, C_m = 7–10 mF m^{-2}, σ_{ih} = 0.75–0.9 S m^{-1}, ε_{ih} = 50–60 ε_0, f_{di} = 21.2–26.5 MHz). Introduction of a distribution of relaxation times (parameter $\alpha = 0.5$, Eq. 6) significantly improves the fit of the spectrum obtained at the conductivity of 0.47 S m^{-1} (Fig. 3, curve 1). For fitting the rotation spectra of generative cells (Fig. 1*A* and Fig. 3, curve 2), the following parameters were assumed: C_m = 7.0–8.5 mF m^{-2}, G_m = 30–400 S m^{-2}, σ_{il} = 0.4 S m^{-1}, σ_{ih} = 0.65 S m^{-1}, ε_{ih} = 75 ε_0, f_{di} = 14.5 MHz, α = 0.5, resulting in the correlation coefficients higher than 0.98. This demonstrates the applicability of Model 2 in analyzing the electrorotational behavior of the generative cells and protoplasts observed over the wide range of external conductivity used in this study.

Electrorotation of Pollen Grains

Electrorotation spectra of pollen grains at various conductivities (Fig. 4) can be fitted very accurately by a superposition of three or four Lorentzian curves (Eq. 7) whose peak parameters (f_{ci} and R_i with i = 1, 2, 3, 4) are listed in Table 1. The characteristic frequencies and magnitudes of the rotation peaks strongly depended on the external conductivity. Under low-conductivity conditions ($\sigma_e < 20$ mS m^{-1}), pollen grains rotated much

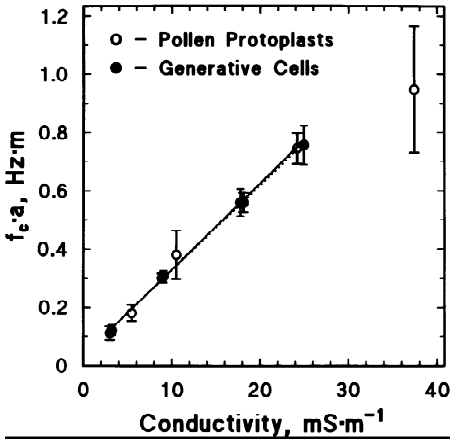

Fig. 2. Cumulative plot of the characteristic anti-field frequency (f_{c1}) normalized to the cell radius (a) versus the external conductivity (σ_e). Measurements were performed on protoplasts (open circles, a = 42.9 ± 4.5 μm, mean ±SD, n = 200) and on generative cells (solid circles, a = 13.9 ± 3.0 μm, n = 120) using the ''null-frequency'' method (*see* Materials and Methods). Each symbol represents a mean ($f_{c1} \cdot a$)-value (±SD) from 20–40 cells measured at closely similar conductivities. The data obtained at conductivity lower than 26 mS m^{-1} were fitted by Eq. 5 (lines). The area-specific membrane parameters (±SE of the fitting) were found to be: for protoplasts (solid line) C_m = 10.8 ± 0.2 mF m^{-2} and G_m = 56 ± 11 S m^{-2}; for generative cells (dashed line) C_m = 10.9 ± 0.2 mF m^{-2} and G_m = 167 ± 33 S m^{-2}.

slower than protoplasts and generative cells (Figs. 1 and Fig. 4*A*, *see also* Table 1). Furthermore, in contrast to the protoplasts and generative cells (Fig. 1*AB*, curves 2), the rotation spectra of pollen grains observed at the lowest conductivity exhibited at least two well resolved antifield maxima (Fig. 4*A*). Apparently, the main reason for the occurrence of the additional high-frequency antifield peak is the complex multishell structure of the pollen grain wall. For both protoplasts and pollen grains, the low-frequency peak (f_{c1}/R_1) is obviously due to the capacitive charging of the plasmalemma (the f_{c1}/R_1-parameters are most sensitive to the C_m/G_m-values independent of the theoretical model). With increasing external conductivity, the f_{c1}-values of pollen grains increased less, from 8.6 kHz (σ_e = 3 mS m^{-1}) to 107 kHz (σ_e = 450 mS m^{-1}), than the f_{c1}-values of protoplasts (2.9 kHz at 3 mS m^{-1} and 134 kHz at 450 mS m^{-1}).

It is well known that the total number of separate peaks or shoulders measured at different external conductivities corresponds to the minimum number of dielectrics or dispersion phenomena of the biological object that have to be considered for correct modeling. Modeling the rotation spectra of the pollen grains of *Lilium longiflorum* on the basis of a two-shell model with the plasma membrane and a homogeneous, nondispersive, ''wall'', and on the basis of Model 2 demonstrated that there were no biologically reasonable parameters which fitted the experimental data. In contrast, a good agreement between the experimental spectra and the theory was found if a three-shell model was used. These three shells are: the plasma membrane (shell 1), the intine (shell 2) and the exine (shell 3). The average thickness of the intine (1 μm) and exine (0.2 μm) of pollen grains used for curve fitting was measured by electron microscopy. Curve-fitting based on Model 2 (protoplasts and generative cells) and Model 3 (pollen grains) yields similar values for the scaling factor, χ. The scaling factor decreased gradually from 1.7–1.5 to 1.1–1.0 as the external conductivity increased from 3–20 mS m^{-1} to 0.46–0.48 S m^{-1} (Table 2).

Discussion

Generative Cells and Protoplasts

Under the osmotic conditions used here (700 mOsm), the generative cells isolated from lily pollen were spherical with a mean radius ±SD of 13.9 ± 3.0 μm, which was estimated for the cell sample (n = 120) shown in Fig. 2. Our data are close to those (15 μm) obtained on the generative cells suspended in a medium of lower (500 mM sucrose) tonicity (Tanaka, 1988). As expected from the van't Hoff law, cells with radius of 15 μm at 500 mOsm would reduce their radius to 13.4 μm after exposure to 700 mOsm.

Within pollen grains and within isolated protoplasts of *Lilium*, the generative cell is surrounded by a callose cell wall, which is enclosed by two cell membranes, the inner of the generative cell and the outer of the vegetative cell (Tanaka et al., 1989). The data on the membrane capacitance reported here (Figs. 1–3) clearly show that *isolated* generative cells were surrounded by a single

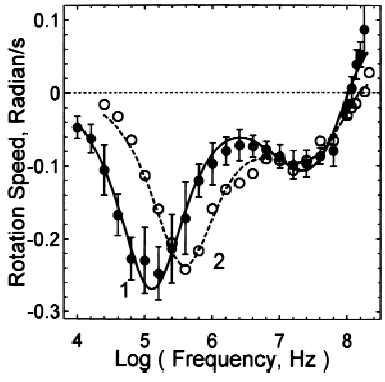

Fig. 3. Rotation spectra of the isolated generative cells (open circles) and protoplasts (filled circles) measured in media of relatively high conductivity, σ_e (0.47–0.48 S m^{-1}). The solid and dashed curves show best fits of Model 2 to the rotation spectra of protoplasts and generative cells, respectively. Model 2 with a distribution of relaxation times (α) provides a much better fit to the experimental spectra. For curve fitting we used values for the various parameters listed in Table 2.

Table 2. *Dielectric properties of the Lilium* pollen wall, membrane and cytosol extracted from electrorotation spectra (Figs. 1, 3, and 4) using Model 2 (the isolated generative cells and protoplasts) and Model 3 (the intact pollen grains)

σ_e mS m^{-1}	Radius μm	n	Exine		Intine		Membrane		Cytoplasm					χ
ε_e = 78.5			σ S m^{-1}	ε	σ S m^{-1}	ε	G_m S m^{-2}	C_m mF m^{-2}	σ_1 S m^{-1}	σ_h S m^{-1}	f_d MHz	α	ε_h	
Generative Cells														
3	16	1					30	7.5	0.4	0.60	14.5	0.5	75	1.52
19	15	4					400	8.5	0.4	0.60	14.5	0.5	75	1.52
480	15	4					100	8.0	0.4	0.65	14.5	0.5	75	1.03
Pollen Protoplasts														
3	48	7					40	8.5	0.375	0.75	26.5	0.5	60	1.55
19	53	3					250	10	0.375	0.75	26.5	0.5	60	1.61
166	45	10					200	9.0	0.375	0.90	21.2	0.4	50	1.20
470	50	5					200	7.0	0.375	0.75	26.5	0.5	60	1.14
Pollen Grains**														
3	50	8	0.0003	20	0.5	70	50	10	0.35	0.9	25.0	0.4	50	1.70
19	53	6	0.0004	15	0.7	70	50	10	0.40	0.9	25.0	0.4	50	1.34
186	52	4	0.0012	15	0.7	70	20	9.0	0.40	0.90	26.0	0.4	50	1.03
460	53	3	0.0030	20	0.6	65	50	8.0	0.45	1.10	27.5	0.5	50	0.95

* The thickness of the exine and of the intine were estimated from electron micrographs to be 0.2 and 1 μm, respectively.

** The effective radius of pollen grains (a_e) is taken as the radius of a sphere with the same total volume as the elongated ellipsoid of revolution, $a_e = (a_l \cdot a_s^2)^{1/3}$, where $a_l \cdot$ and a_s are the long and short semiaxes of the particle, respectively.

membrane. The C_m values of 0.7–1.1 mF m^{-2} are in good agreement with values accepted as typical for single biological membranes (Pething & Kell, 1987; Schwan, 1988). A double membrane structure (two close lipid membranes in series) would yield a much lower values for the apparent C_m determined on the basis of the single-shell model (Model 1, Eq. 5). The ultrastructural observations also reveal that generative cells tend to round up and to lose their outer membrane during isolation (Tanaka et al., 1989). The apparent membrane conductivity, G_m, of the generative cells (173 S m^{-2}) obtained from the $(f_{c1}a)/\sigma_e$-data (Fig. 2) using the single-shell model (Eq. 5) is much higher than the usual range for biomembranes. The discrepancy is presumably due to the presence of an additional shell, a callosic cell wall (Tanaka, 1988), because we did not use any enzyme treatment for preparation of the generative cells from pollen protoplasts. A highly conductive, thin surface layer (such as a cell wall or a glycocalix) will cause a significant tangential, surface conductance (K_S) in small-sized cells and will, therefore, lead to an overestimation of the membrane conductivity evaluated on the basis of the single-shell model (Fuhr & Kuzmin, 1986; Hu, Arnold & Zimmermann, 1990; Sukhorukov, Arnold & Zimmermann, 1993).

Although the single-shell model matches well the experimental spectra of protoplasts and generative cells at low conductivities (Figs. 1–2), the occurrence of two antifield peaks at higher conductivities (Fig. 3) is inconsistent with this model. This demonstrated that rotation spectra must be taken at several conductivities before selecting or rejecting a model. The changes in the rotation spectra of isolated protoplasts and generative cells with increasing conductivity could be modeled very well by assuming dispersion of the cytoplasm. The magnitude ($\Delta\sigma_i$) and frequency (f_d) of dispersion reflect the electrical properties, size, concentration and other parameters of cytoplasmic organelles and macromolecules (for mechanisms of dielectric dispersion *see* Pethig & Kell (1987) and Schwan (1988)). The dispersion parameters, $\Delta\sigma_i$ and f_d, could be extracted from the rotation spectra if the external conductivity approached that of the cytoplasm (Fig. 3). The cytoplasm of generative cells exhibited dielectric dispersion centered at 14.5 MHz, whereas the cytoplasm of protoplasts dispersed at higher frequency (26.5 MHz). Introduction of the relaxation time spread parameter ($\alpha = 0.5$, in Eqs. 6 *a* and *b*) significantly improved the fit of Model 2 to the experimental data obtained on both protoplasts and generative cells (Fig. 3), indicating several polarization mechanisms that contributed to the dielectric response of the cytoplasm of both cell types. Examination of the ultrastructure of intact pollen grains and of isolated vegetative-cell-protoplasts (Takana et al., 1989) revealed that the vegetative cell of lily pollen contains a large number of vesicles and organelles of different size (nucleus, mitochondria, amyloplasts, lipid bodies etc.). The spindle-shaped generative cell (*see* above) is also suspended in the cytoplasm of protoplasts. All these cellular components obviously contributed to the internal dispersion of

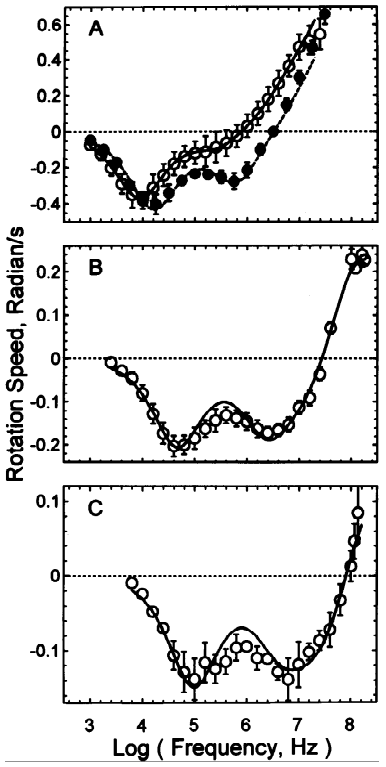

Fig. 4. Rotation spectra of intact pollen grains of *Lilium longiflorum* measured in media of increasing conductivity. (*A*) The rotation spectra were taken at 3 mS m^{-1} (open circles) and at 19 mS m^{-1} (filled circles), respectively. The rotation spectra shown in *B* and *C* were measured at conductivities of 0.19 and 0.46 S m^{-1}, respectively. The curves represent best fits of the three-shell model (Model 3) to the data (for details *see* Table 2).

vegetative cells giving rise to a superposition of various relaxation processes around the mean frequency of 26.5 MHz. In addition, proteins, nucleic acids and other macromolecules also disperse via different mechanisms over the MHz frequency range (Hasted, 1973; Hedvig, 1977; Pethig & Kell, 1987; Gimsa et al., 1996).

In contrast to the cytoplasm of vegetative cells, there are much less organelles in the cytoplasm of generative cells (Tanaka et al., 1989). The absence of these relatively small sized organelles would explain the lower value of f_d (14.5 MHz) deduced for the cytoplasm of generative cells. Because the dispersion frequency is inversely proportional to the radius (a) of organelles (Hasted, 1973; Schwan, 1988): $f_d = (\sigma_i + aG_m)/(2\pi aC_m)$, where G_m and C_m are membrane conductance and capacitance per unit area; σ_i is the internal conductivity, that is usually much higher than the product $(a \cdot G_m)$. The internal dispersion of generative cells can be partly attributed to highly condensed chromatin detected in their relatively large nucleus (Tanaka, 1989). The value of the high-frequency internal conductivity of the generative cells (σ_{ih} = 0.6–0.65 S m^{-1}) was found to be slightly lower than that of the protoplasts (0.75–0.9 S m^{-1}). This may be interpreted as resulting either from lower ionic content or higher viscosity of the cytoplasm of generative cells. (The cytoplasm of generative cells is generally more electron-dense than that of the vegetative cell (Tanaka et al., 1989)).

Pollen Grains

To explain the complex rotation spectra of pollen grains in terms of the conductivities and permittivities of their components (Fig. 4), we tested whether the rotational behavior of pollen grains followed one of the theoretical models for layered spherical particles. Despite the slightly elongated shape of pollen grains, their rotation spectra obtained at various external conductivities could be fitted with a three-shell, spherical model (curves in Fig. 4). According to this model, the pollen grain consists of four layers with different electrical properties related to the chemical composition and other characteristics of the four dielectrics. The layered structure of lily pollen was readily seen in transmission electron micrographs. The principal material of the outermost layer (shell 1), the exine, is a highly resistant, hydrophobic wall polymer, sporopollenin, which is resolved into a lipid and a lignin-like fraction (Southworth, 1990; Stanley & Linskens, 1974). The inner cell wall (shell 2), the intine, shows a rather uniform thickness (about 1 μm), and consists of the hydrophilic polysaccharides, pectin and cellulose (Tanaka et al., 1989; Heslop-Harrison & Heslop-Harrison, 1991). Shell 3 and the innermost layer in the theoretical model correspond to the plasma membrane and the cytosol of the vegetative cell, respectively. The rotation measurements on isolated pollen protoplasts (*see* above) significantly facilitated the evaluation of the electrical parameters of intact pollen grains. The three-shell model allowed biologically reasonable values for the conductivity and permittivity of the wall (exine and intine), the membrane and the cytosol of pollen grains to be deduced by curve fitting. However, the model is only a rough approximation, because it neglects some structural characteristics of the *Lilium* pollen, such as the multiple strata (sexine, nexine etc.) and the reticulate pattern of the exine, and further peculiarities of the outermost layer (e.g., the extremely nonuniform thickness, the bacula and capita of the sexine, etc.) (Sheldon & Dickinson, 1983; Takahashi, 1995; Schmid, Eberwein & Hesse, 1996).

The values of the exine permittivity reported here (ε = 15–20) are in good agreement with those (ε = 30) obtained on pollen of *Pinus strobus* (Müller et al., 1993) by means of electrorotation. The exine conductivity in lily pollen grew gradually from 0.3 to 3 mS m^{-1} with increasing conductivity of the medium (Fig. 4, Table 2). Similar effects of medium salinity on the conductivity

of the cell wall were reported for yeast cells (Asami & Yonezawa, 1996). The value of exine conductivity (σ_{exine} = 0.3 mS m^{-1}) obtained at the lowest external conductivity used in this study (3 mS m^{-1}) is higher than that derived for the pollen of *Pinus strobus* (σ_{exine} = 0.05 mS m^{-1}) at the external conductivity of 1 mS m^{-1} (Müller et al., 1993). The relatively low values of the exine conductivity and permittivity reveal a very poor porosity (and consequently, low water and ion concentrations) of this outer cuticularized wall layer, whose principal function is the prevention of water loss. The values of the exine conductivity and permittivity obtained here can be expected for the reported composition of the exine that consists of the fatty acid-lignin-like dense polymer, sporopollenin, and is impregnated with oily substances (Heslop-Harrison, 1968; Southworth & Branton, 1971).

The inner, porous cell wall of lily pollen, the intine, is mostly formed of the hydrophilic polysaccharides, pectin and cellulose (Heslop-Harrison & Heslop-Harrison, 1991). As expected the intine was found to be much more conductive (σ_{intine} = 0.5–0.7 S m^{-1}, ε_{intine} = 65–70, *see* Table 2) than the exine. The σ_{intine} value was independent of the salinity of the external medium, and it did not noticeably change during prolonged incubation (up to 2 hr) under extremely low-salinity conditions (3 mS m^{-1}). These results suggest that ion exchange between the intine and the outer medium occurs very slowly, apparently, due to a very poor ionic permeability of the exine. The σ_{intine} value of lily pollen obtained in this work is much higher than the σ-value (3.5 mS m^{-1}) obtained for the intine of *Pinus strobus* (Müller et al., 1939). The discrepancy (*see* also the σ_{exine} values) may be due to the difference in the pollen wall composition between the angiosperm *Lilium longiflorum* and the gymnosperm *Pinus strobus* (Stanley & Linskens, 1974).

The values of C_m and G_m assumed for the plasma membrane of intact pollen grains are consistent with those estimated for isolated protoplasts (Figs. 1–3), whereas the internal conductivity (σ_{ih} = 0.9–1.1 S m^{-1}) of pollen grains was somewhat higher than the σ_{ih} values (0.75–0.9 S m^{-1}) obtained on isolated protoplasts. Lower values for the internal conductivity of isolated protoplasts may be due to their osmotic swelling and due to ion leakage from the cytoplasm induced by the harsh enzymatic treatment used for protoplast isolation. A similar decrease in the internal conductivity has been observed by electrorotation of yeast cells and yeast protoplasts (Radu et al., 1996).

Conclusion

Electrorotation measurements performed over a wide range of medium conductivity enabled a detailed analysis of the dielectric spectra of isolated gamete cells and of intact lily pollen using theoretical, single and multiple shell models. The interpretation of complex rotation spectra of pollen grains was markedly facilitated by using the parameters obtained on isolated pollen protoplasts. For intact pollen grains, electrorotation allowed the evaluation of the electric properties in terms of conductivities and permittivities of the different layers of the pollen grain envelope (the exine, intine and plasma membrane) and the average properties of the cytosol. These electrical parameters are useful for estimation of ionic concentrations, permeabilities and further important biological characteristics of the pollen grain compartments.

In the present study electrorotation was proved to be able to characterize individual pollen grains and their major structural units, and therefore, electrorotation can be employed as an important diagnostic technique in pollen-related studies, including studies on plant reproduction and plant breeding. The electrical parameters of pollen obtained by means of electrorotation can also be useful in analyzing changes in pollen viability upon storage or upon exposure to toxic substances, electromagnetic radiations etc.

We thank Prof. G. Fuhr (Humboldt-University, Berlin, Germany) for providing microstructured rotation chambers. We are grateful to Dr. M. Höftberger (University of Salzburg, Austria) for electron microphotographs of pollen and to Ms. E. Horn for her skillful technical assistance. This work was supported by grants of the Deutsche Forschungsgemeinschaft (Stipendium No. 1786/1-1 to R.B.; SFB 176, project B5 to U.Z.) and of the VDI/VDE (13MV 0305) to U.Z.

References

Arnold, W.M., Schwan, H.P., Zimmermann, U. 1987. Surface conductance and other properties of latex particles measured by electrorotation. *J. Phys. Chem.* **91:**5093–5098

Arnold, W.M., Zimmermann, U. 1982. Rotating-field-induced rotation and measurement of the membrane capacitance of single mesophyll cells of *Avena sativa. Z. Naturforsch.* **37:**908–915

Arnold, W.M., Zimmermann, U. 1988. Electro-rotation: development of a technique for dielectric measurements on individual cells and particles. *J. Electrostatics* **21:**151–191

Asami, K., Yonezawa, T. 1996. Dielectric behavior of wild-type yeast and vacuole-deficient mutant over a frequency range of 10 kHz to 10 GHz. *Biophys. J.* **71:**2192–2200

Battey, N.H., Blackbourn, H.D. 1993. The control of exocytosis in plants. *New Phytol.* **125:**307–338

Cai, G., Moscatelli, A., Cresti, M. 1997. Cytoskeletal organization and pollen tube growth. *Trends in Plant Sci.* **2:**86–91

Cresti, M., Blackmore, S., Van Went, J.L. 1992. Atlas of Sexual Reproduction in Flowering Plants. Springer-Verlag, New York

Feijó, J.A., Malhó, R., Obermeyer, G. 1995. Ion dynamics and its possible role during in vitro germination and tube growth. *Protoplasma* **187:**155–167

Fuhr, G., Kuzmin, P.I. 1986. Behavior of cells in rotating electric fields with account to surface charges and cell structures. *Biophys. J.* **50:**789–795

Fuhr, G., Zimmermann, U., Shirley, S.G. 1996. Cell motion in time-varying fields: Principles and potential. *In:* Electromanipulation of Cells. U. Zimmermann and G.A. Neil, editors. pp. 259–328. CRC Press, Boca Raton, Florida

Gascoyne, P.R.C., Becker, F.F., Wang, X.-B. 1995. Numerical analysis of the influence of experimental conditions on the accuracy of dielectric parameters derived from electrorotation measurements. *Bioelectrochem. Bioenerg.* **36:**115–125

Gimsa, J., Müller, T., Schnelle, T., Fuhr, G. 1996. Dielectric spectroscopy of single human erythrocytes at physiological ionic strength: Dispersion of the cytoplasm. *Biophys. J.* **71:**498–506

Harold, J.M., Caldwell, J.H. 1990. Tips and current: Electrobiology of apical growth. *In:* Tip Growth in Plant and Fungal Cells. I.B. Heath, editor. pp. 59–90. Academic Press, San Diego

Hasted, J.B. 1973. Aqueous Dielectrics. Chapman and Hall Ltd., London

Heath, I.B. 1995. Integration and regulation of hyphal tip growth. *Can. J. Bot.* **73:** (Suppl.) S131–S139

Hedvig, P. 1977. Dielectric Spectroscopy of Polymers. Adam Hilger Ltd., Bristol

Heidemann, S.R. 1996. Cytoplasmic mechanism of axonal and dendritic growth in neurons. *Int. Rev. Cytol.* **165:**235–296

Heslop-Harrison, J. 1968. Pollen wall development. *Science* **161:**230–237

Heslop-Harrison, J., Heslop-Harrison, Y. 1991. Structural and functional variations in pollen intine. *In:* Pollen and Spores. S. Blackmore and S.H. Barnes, editors. pp. 331–343. Clarendon Press, Oxford

Hu, X., Arnold, W.M., Zimmermann, U. 1990. Alteration in the electrical properties of T and B lymphocyte membranes induced by mitogenic stimulation. Activation monitored by electro-rotation of single cells. *Biochim. Biophys. Acta* **1021:**191–200

Jones, T.B. 1995. Electromechanics of Particles. Cambridge University Press, New York

Kühtreiber, W.M., Jaffe, L.F. 1990. Detection of extracellular calcium gradients with a calcium-sensitive vibration electrode. *J. Cell Biol.* **110:**1565–1573

Miller, D.D., Callaham, D.A., Gross, D.J., Hepler, P.K. 1992. Free Ca^{2+} gradient in growing pollen tubes of *Lilium. J. Cell Sci.* **101:**7–12

Mishra, K.P., Joshua, D.C., Bhatia, C.R. 1987. In vitro electroporation of tobacco pollen. *Plant Sci.* **52:**135–139

Müller, T., Küchler, L., Fuhr, G., Schnelle, Th., Sokirko, A. 1993. Dielektrische Einzelzellspektroskopie an Pollen verschiedener Waldbaumarten—Charakterisierung der Pollenvitalität. *Silvae Genetica* **42:**311–322

Nielsen, K., Schenk, W.A., Kriegmaier, M., Sukhorukov, V.L., Zimmermann, U. 1996. Absorption of tungsten carbonyl anions into the lipid bilayer membrane of mouse myeloma cells. *Inorg. Chem.* **35:**5762–5763

Obermeyer, G., Bentrup, F.-W. 1996. Regulation of polar cell growth and morphogenesis. *Prog. Botany* **57:**54–67

Obermeyer, G., Lützelschwab, M., Heuman, H.-G., Weisenseel, M.H. 1992. Immunolocalization of H^+ ATPases in the plasma membrane of pollen grains and pollen tubes of *Lilium longiflorum. Protoplasma* **171:**55–63

Obermeyer, G., Weisenseel, M.H. 1991. Calcium channel blocker and calmodulin antagonists affect the gradient of free calcium ions in lily pollen tubes. *Eur. J. Cell Biol.* **56:**319–327

Obermeyer, G., Weisenseel, M.H. 1995. Introduction of impermeable molecules into pollen grains by electroporation. *Protoplasma* **187:**132–137

Pastushenko, V.Ph., Kuzmin, P.I., Chizmadzhev, Yu.A. 1985. Dielectrophoresis and electrorotation—a unified theory of spherically symmetrical cells. *Studia biophysica* **110:**51–57

Pauly, H., Schwan, H.P. 1959. Über die Impedanz einer Suspension von kugelförmigen Teilchen mit einer Schale. Ein Modell für das dielektrische Verhalten von Zellsuspensionen und von Proteinlösungen. *Z. Naturforsch.* **14b:**125–131

Pethig, R., Kell, D.B. 1987. The passive electrical properties of biological systems: the significance in physiology, biophysics and biotechnology. *Phys. Med. Biol.* **32:**933–977

Pierson, E.S., Miller, D.D., Callaham, D.A., Shipley, D.A., Rivers, B.A., Cresti, M., Hepler, P.K. 1995. Pollen tube growth is coupled to the extracellular ion flux and the intracellular calcium gradient: Effect of BAPTA-type buffers and hypertonic media. *Plant Cell* **6:**1815–1828

Plätzer, K., Obermeyer, G., Bentrup, F.-W. 1997. AC fields of low frequency and amplitude stimulate pollen tube growth possibly via stimulation of the plasma membrane proton pump. *Bioelectrochem. Bioenerg.* (*in press*)

Radu, M., Petcu, I., Sommer, A., Avram, D. 1996. Changes in membrane electrical parameters of yeast following chemical treatment for protoplast isolation. *Bioelectrochem. Bioenerg.* **40:**159–166

Saunders, J.A., Matthews, B.F., Wert, S.V. 1992. Pollen electrotransformation for gene transfer in plant. *In:* Guide to Electroporation and Electrofusion. D.C. Chang, B.M. Chassy, J.A. Saunders, A.E. Sowers, editors. pp. 227. Academic Press, San Diego

Saunders, J.A., Lin, C.H., Hou, B.H., Cheng, J., Tsengwa, N., Lin, J.J., Smith, C.R., McIntosh, M.S., Wert, S.V. 1995. Rapid optimization of electroporation conditions for plant cells, protoplasts, and pollen. *Mol. Biotechnol.* **3:**181–190

Schmid, A.-M.M., Eberwein, R.K., Hesse, M. 1996. Pattern morphogenesis in cell walls of diatoms and pollen grains: a comparison. *Protoplasma* **193:**144–173

Schwan, H.P. 1988. Dielectric spectroscopy and electro-rotation of biological cells. *Ferroelectrics* **86:**205–233

Sheldon, J.M, Dickinson, H.G. 1983. Determination of patterning in the pollen wall of *Lilium henryi. J. Cell Sci.* **63:**191–208

Sokirko, A.V. 1992. The electrorotation of axisymmetrical cell. *Biol. Mem.* **6:**587–600

Southworth, D. 1990. Exine biochemistry. *In:* Microspores: Evolution and Ontogeny. S. Blackmore and R.B. Knox, editors. pp. 193–212. Academic Press, London

Southworth, D., Branton, D. 1971. Freeze-etched pollen walls of *Artemisia pycnocephala* and *Lilium humboldtii. J. Cell Sci.* **9:**193–207

Stanley, R.G., Linskens, H.F. 1974. Pollen-Biology, Biochemistry, Management. Springer-Verlag, Berlin, Heidelberg, New York

Sukhorukov, V.L., Arnold, W.M., Zimmermann, U. 1993. Hypotonically induced changes in the plasma membrane of cultured mammalian cells. *J. Membrane Biol.* **132:**27–40

Sukhorukov, V.L., Zimmermann, U. 1996. Electrorotation of erythrocytes treated with dipicrylamine: Mobile charges within the membrane show their ''signature'' in rotational spectra. *J. Membrane Biol.* **153:**161–169

Takahashi, M. 1995. Three-dimensional aspects of exine initiation and development in *Lilium longiflorum. Am. J. Bot.* **82:**847–854

Tanaka, I. 1988. Isolation of generative cells and their protoplasts from pollen of *Lilium longiflorum. Protoplasma* **142:**68–73

Tanaka, I., Nakamura, S., Miki-Hirosige H. 1989. Structural features of isolated generative cells and their protoplasts from pollen of some liliaceous plants. *Gamete Res.* **24:**361–374

Wang, C., Rathore, K.S., Robinson, K.R. 1989. The responses of pollen to applied electrical fields. *Dev. Biol.* **136:**405–410

Wang, J., Sukhorukov, V.L., Djuzenova, C.S., Zimmermann, U., Müller, T., Fuhr, G. 1997. Electrorotational spectra of protoplasts generated from the giant alga *Valonia utricularis*. *Protoplasma* **196:**123–134

Weisenseel, M.H., Nuccitelli, R., Jaffe, L.F. 1975. Large electrical currents traverse growing pollen tubes. *J. Cell Biol.* **66:**556–567

Wolfram, S. 1991. Mathematica. A System for Doing Mathematics by Computer. 2nd Edition. Adisson-Wesley, Redwood City, California

Zimmermann, U., Arnold, W.M. 1983. The interpretation and use of the rotation of biological cells. *In:* Coherent Excitations in Biological Systems. H. Fröhlich and F. Kremer, editors. pp. 211–221. Springer-Verlag, Berlin

Zimmermann, U. 1982. Electric field-mediated fusion and related electrical phenomena. *Biochim. Biophys. Acta* **694:**227–277

Zimmermann, U. 1986. Electrical breakdown, electropermeabilization and electrofusion. *Rev. Physiol. Biochem. Pharmacol.* **105:**175–256

Zimmermann, U. 1996. Electrofusion of cells: State of the art and future directions. *In:* Electromanipulation of Cells. U. Zimmermann and G.A. Neil, editors. pp. 173–258. CRC Press, Boca Raton, FL